

# High Weibull Modulus HVOF Titania Coatings

R.S. Lima and B.R. Marple

(Submitted 15 January 2002; in revised form 30 March 2002)

The mechanical behavior of high-velocity oxyfuel (HVOF) sprayed titania ( $\text{TiO}_2$ ) coatings was evaluated using Vickers hardness measurements on the cross section and top surface. The distribution of hardness values for the cross-section and top surface under 25, 50, 100, 300, 500, and 1000 g loads was analyzed via Weibull statistics. The coating microstructure was evaluated using scanning electron microscopy (SEM). It was observed that the microstructural features were similar in the top surface and cross-section, different from the lamellar structure commonly found in thermal spray coatings. X-ray diffraction (XRD) analysis identified rutile as the major coating phase. The in-flight sprayed particle parameters such as temperature and velocity were determined using a commercial diagnostic system based on pyrometry and time-of-flight measurements. The uniformity of the microstructure resulted in a near isotropic behavior of the mechanical properties, such as hardness, in the coating cross-section and top surface. High Weibull modulus values were observed when compared with results of other thermal spray coatings available in the literature. These initial results should contribute to a more general understanding of the conditions necessary to achieve coatings with high uniformity and assist in the engineering of coating microstructures for specific applications.

**Keywords** hardness, high-velocity oxyfuel, titania, tailoring of microstructures, Weibull modulus

## 1. Introduction

The engineering of thermal spray coatings for specific applications through the optimization of the conditions and parameter values is a major component of the coating development process. This procedure is often one of trial and error, involving the production of a large number of samples followed by extensive characterization and testing. It is normally a long and expensive process. Developing a broader knowledge of the thermal spray coating microstructure, and its relationship with various properties will help in this engineering process by providing tools that will aid in predicting how process changes will affect the microstructure and properties. Also of prime importance for engineering thermal spray coatings is an understanding of the effect of the feedstock morphology and features on the coating microstructure and the in-flight characteristics of temperature ( $T$ ) and velocity ( $V$ ) of the sprayed particles.

Many advances have been made in the thermal spray field in the last few years: introduction of HVOF and cold-spray development, in-flight particle diagnostic systems, improvement of plasma systems, and the availability of nanostructured feedstocks. However, despite these improvements and innovations, the majority of papers available in the thermal spray literature provide little direction and insight regarding how to engineer a coating.

By analyzing a majority of the papers dealing with mechanical properties of thermal spray coatings, one can observe that measured properties, such as elastic modulus, hardness, fracture toughness, and adhesion/cohesion, are normally reported only as

average values together with a standard deviation. The microstructure of thermal spray coatings is quite complex.<sup>[1-3]</sup> The coating properties will be affected by many different types of interactions, from the coating phases to the splat-splat contact (fine pores). Average and standard deviation are not enough to delineate, represent, understand, and mainly engineer this inhomogeneous system.

Berndt and McPherson,<sup>[4]</sup> Ostojic and McPherson,<sup>[5]</sup> Lin and Berndt,<sup>[6]</sup> and Leigh et al.<sup>[7]</sup> were pioneers in applying the concept of Weibull distribution to analyze the variability of adhesion/cohesion, fracture toughness, hardness, and elastic modulus, respectively, of thermal spray coatings. The Weibull distribution has been used successfully to describe a wide range of problems, including the mechanical properties of brittle materials and lifetime testing. Lima et al. showed that coatings with the same composition could have similar values of hardness (i.e., average and standard deviation) but significantly different Weibull modulus behavior.<sup>[8]</sup> This characteristic should affect coating performance.

One other factor that creates difficulties in engineering thermal spray coatings is the lack of data on properties measured on the top surface. Generally, the coating properties are measured on the cross-section. As thermal spray coatings are normally anisotropic,<sup>[1-3]</sup> knowledge of properties in both directions is very important, particularly for developing more reliable computer modeling approaches. Leigh et al.,<sup>[7,9]</sup> Margadant et al.,<sup>[10]</sup> and Buchmann and Gadw<sup>[11]</sup> are a few of the recent references available in the literature with data taken on the top surface and cross-sections of thermal spray coatings.

The current study focused on producing titania coatings by HVOF thermal spraying. One of the most promising applications of titania thermal spray coatings is in the biomedical area. Titania is a bioinert material and can be used as a bond coat for hydroxyapatite<sup>[12,13]</sup> on titanium-based hip joints, knee prosthetics, and dental root implants. Hydroxyapatite is a biocompatible material, which promotes integration between the titanium-based alloys and the bone tissue. However, its low mechanical strength affects the lifetime of the prosthetics, lead-

R.S. Lima and B.R. Marple, National Research Council of Canada, 75 De Mortagne Blvd, Boucherville, QC J4B 6Y4, Canada. Contact e-mail: rogerio.lima@CNRC-NRC.gc.ca.

ing to more frequent replacement and disruptions in the life of the patient. Incorporating thermal spray titania as a bond coat layer may help in improving the mechanical properties of hydroxyapatite coatings.<sup>[12, 13]</sup> Due to the very delicate nature of this kind of coating application (human life), a detailed knowledge of the microstructural features of titania coatings is of great importance. For this type of application, computational simulations might be an important tool in predicting and engineering coating properties and in increasing the lifetime of prosthetics. As a consequence, improving the understanding of the mechanical properties of titania coatings is fundamental for any future experimental and/or modeling work.

This work attempts to identify the factors that contribute to producing HVOF-sprayed coatings of titania with high Weibull modulus values of hardness. Hardness values and their respective Weibull modulus values were determined over a range of indentation loads on the top surface and cross-section of titania coatings. Some considerations on the transition point between load-dependent hardness and constant hardness will be presented.

## 2. Experimental Procedure

A titania ( $\text{TiO}_2$ ) feedstock Amperit 782.0 (H.C. Starck GmbH & Co. KG, Goslar, Germany) with a nominal particle size distribution from 5–22  $\mu\text{m}$  was sprayed on low carbon steel substrates using a DJ 2700 HVOF torch (Sulzer-Metco, Westbury, NY). The spray parameters are listed in Table 1. Typical coating thickness was  $\sim 340 \mu\text{m}$ . Vickers hardness measurements were performed under 25, 50, 100, 300, 500, and 1000 g loads for 15 s on the cross-section and top surface of the coatings. Both the cross-section and top surface were polished before making the indentations. The coefficient of variation (CV) for these measurements stabilized at around 14–17 indentations and, therefore, 20 hardness measurements were taken for each sample. This technique of sample size determination was also used by Lin and Berndt.<sup>[6]</sup> The hardness measurements were evaluated using a Weibull statistical distribution. The results were fitted to the 2-factor Weibull function employing the following probability function ( $P_i$ ):  $P_i = i/(N + 1)$ , where  $N$  is the total number of hardness data points and  $i$  is the  $i$ th order in the ascending data set.<sup>[6]</sup>

The coating microstructure was analyzed by scanning electron microscopy (SEM) on both the cross-section and top surface. X-ray diffraction (XRD;  $\text{Cu K}\alpha$  radiation) was used to determine the phases present. Information on the particle state during coating deposition was obtained to aid in understanding the process. The particle temperature, velocity, and diameter in the spray jet were measured using a diagnostic tool (DPV2000, Tecnar Automation, Saint Bruno, QC, Canada). The DPV2000 unit uses a system based on optical pyrometry and time-of-flight measurements to obtain information on the spray jet. Individual particles are detected in the spray jet to provide temperature, velocity, and particle diameter information. A total of 3000 particles were measured to acquire the data for these three parameters. These in-flight characteristics were determined at the centerline of the HVOF spray jet, where the particle flow density was the highest.

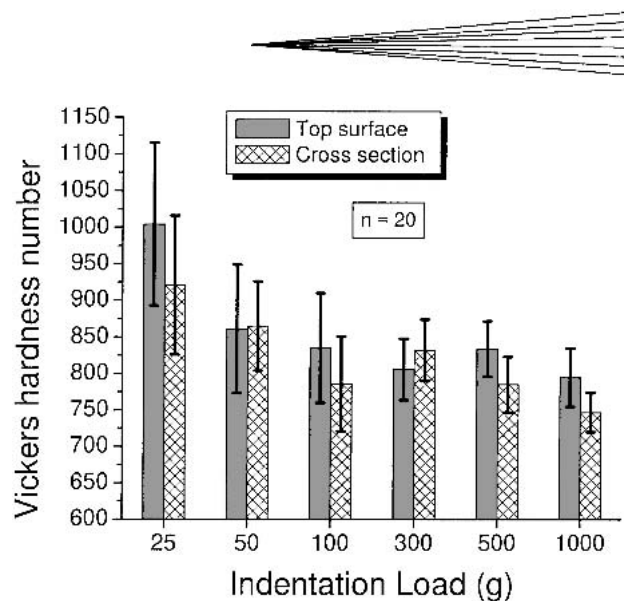


**Fig. 1** Vickers hardness on the top surface and cross section of HVOF titania coatings for different indentation loads

**Table 1** HVOF Parameters for the Titania Feedstock, DJ 2700

Parameter	Value
Propylene flow	132 scfh (62.3 slpm)
Oxygen flow	491 scfh (231.8 slpm)
Air flow	786 scfh (371 slpm)
Carrier gas ( $\text{N}_2$ ) flow	20 scfh (9.4 slpm)
Powder feed rate	30–35 g/min
Spray distance	20 cm

## 3. Results and Discussion

### 3.1 Hardness and Weibull Modulus

Figures 1 and 2 show the Vickers hardness and Weibull modulus values obtained for the top surface and cross-section under different indentation loads. The hardness decreases from  $\sim 900$ –1000 Vickers at an indentation load of 25 g to  $\sim 750$ –800 Vickers at an indentation load of 1000 g, for both the top surface and cross-section. At lower loads, the indentation diagonal sizes are quite small, indicating that only a small region of the coating is being sampled. For example, at an indentation load of 25 g, the indentation diagonal length is approximately 7  $\mu\text{m}$ . This can minimize the extent of defects, such as coarse pores, splat boundaries, and microcracking, enclosed within the indentation. As the indentation load increases, so does the volume of coating being analyzed. For example, at an indentation load of 1000 g, the indentation diagonal length is approximately 50  $\mu\text{m}$ . As a consequence, porosity, splat boundaries and microcracking should play a significant role on hardness, lowering its value. This phenomenon is expected and was also observed in hardness and elastic modulus measurements via indentation techniques in plasma sprayed zirconia coatings.<sup>[14]</sup> Therefore, the mechanical properties of polycrystalline materials exhibit a “size effect.” Mechanical properties measured in low volumes will yield a different behavior than those measured using large sampling volumes. Marshall et al.<sup>[15]</sup> used the Knoop indentation technique to

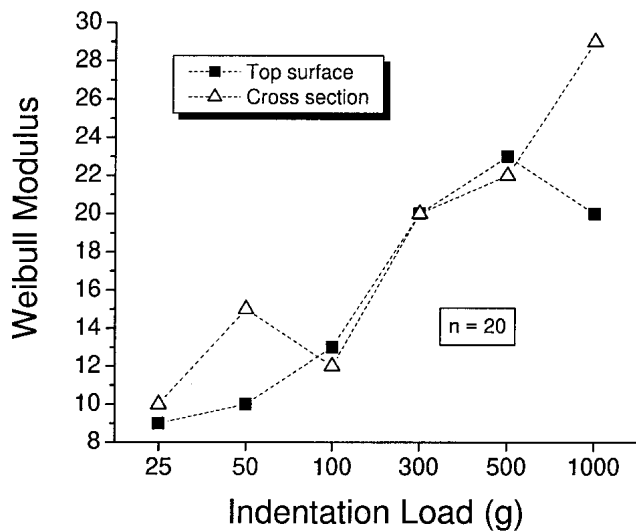


**Fig. 2** Weibull modulus of hardness on the top surface and cross-section of HVOF titania coatings for different indentation loads

measure the elastic modulus of bulk materials. The elastic modulus values obtained via the indentation method were similar to those obtained by other techniques. Wisely, Marshall et al.<sup>[15]</sup> used high indentation loads; i.e., equal to or greater than 1000 g. High indentation loads will make indentation impressions with dimensions larger than the critical area or volume, where the material defects encountered per unit area/volume become relatively constant. After this point is reached, the mechanical property values measured by indentation techniques should be in better agreement with those measured by other methods.

The values of the Weibull modulus of the hardness numbers were calculated and are shown in Fig. 2. The Weibull modulus is a measure of the variability of material strength. Low Weibull modulus values indicate a high variability in strength, and vice-versa. As a general trend, it can be observed in Fig. 2 that the Weibull modulus increases with increasing load. Valente<sup>[16]</sup> observed the same phenomenon for different thermal spray coatings using Vickers indentation at three different loads (100, 300, and 500 g).

At low indentation loads the test volume is small and may be smaller than other material defects, such as pores, splat boundaries, and cracks. As a consequence, the probability of sampling a “low-defect region” becomes higher; thereby yielding high hardness values. However, when one indents on a defective zone, the measured hardness can be much lower. Therefore, at low loads there can be a significant scatter in the data distribution, which is observed in the low Weibull modulus values. On the other hand, at high indentation loads the test volume is large and the probability of finding defects (pores, splat boundaries, cracks) within the volume under scrutiny increases. In other words, each indent tends to encounter a volume representative of the bulk material. This decreases the scatter in the measurements. These more homogeneous measurements are reflected in the higher Weibull modulus values exhibited for higher indentation loads.

The experimental results show the importance of the indentation load when comparing Weibull modulus values of material

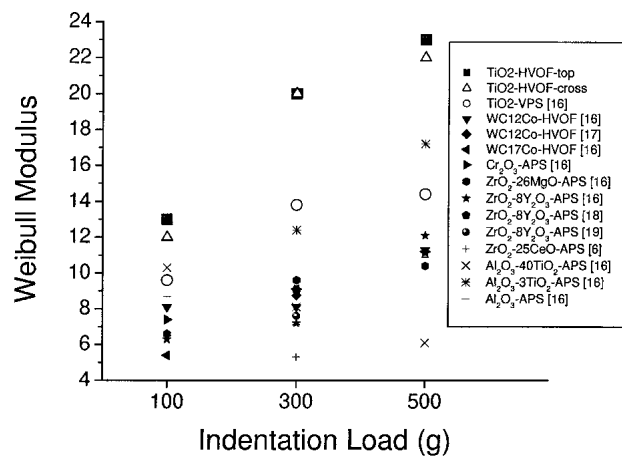


**Fig. 3** Weibull modulus of hardness of HVOF titania and various thermal spray ceramic coatings for different indentation loads. Weibull modulus values of the references were taken from the cross sections

hardness. To compare the variability of material strength of two or more materials through hardness measurements, one must do it by comparing Weibull modulus values obtained at the same load. As a comparison of hardness values obtained from different loads has no significance, the same concept has to be applied for Weibull modulus obtained from indentation measurements. This concept should also be applied to the other mechanical properties that can be measured by indentation techniques, such as elastic modulus.<sup>[14,15]</sup>

Based on this concept, Fig. 3 shows a plot of Weibull modulus values for different thermally sprayed ceramic coatings<sup>[6,16-19]</sup> for indentation loads of 100, 300, and 500 g, including the HVOF titania coatings produced during this work. It can be observed that the Weibull modulus values of the HVOF titania are significantly higher than the general Weibull modulus values for the other ceramic coatings.

From Fig. 4, it can be observed that the hardness values for the titania coatings produced by HVOF and vacuum plasma spray (VPS) processes are similar. Despite the similarity in hardness values for these two groups of coatings, Fig. 3 clearly shows that the values of Weibull modulus for the two coating techniques are different. The HVOF sprayed titania has higher Weibull modulus values than the VPS sprayed titania for all three indentation loads tested (Fig. 3). Lima et al. observed a similar behavior for partially stabilized zirconia (PSZ) coatings.<sup>[8]</sup> A total of five PSZ coatings exhibited similar hardness values but a different behavior of Weibull distribution. Therefore, as Weibull modulus is a measure of the variability of material strength, two or more materials with similar mechanical property values—i.e., average and standard deviation—may be differentiated and compared through their respective Weibull modulus values. The Weibull modulus may be used to determine which material has higher uniformity and reliability. Average and standard deviation per se are not sufficient to characterize the mechanical properties of thermal spray coatings. A statistical analysis such as Weibull distribution is necessary for a more complete understanding of the influence of the microstructure on mechanical properties. It is important to point out that me-

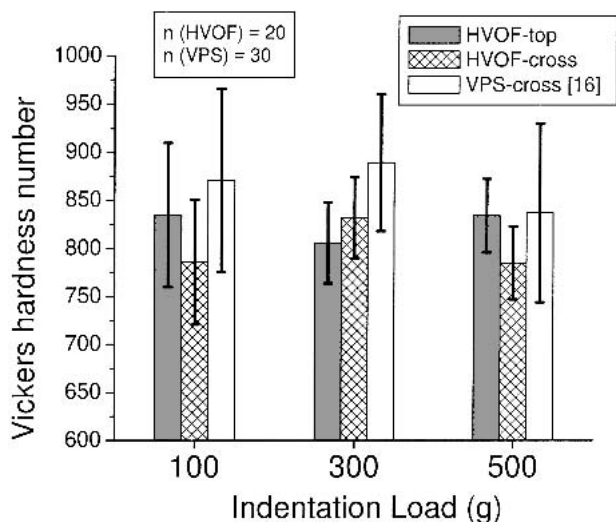


Fig. 4 Hardness values of HVOF and VPS titania coatings for the indentation loads of 100, 300, and 500 g

**Table 2 Top Surface and Cross-Section Vickers Hardness Ratio for Different Ceramic Coatings and Thermal Spray Systems**

Material	Thermal Spray Method	HV Top/HV Cross	Reference
TiO <sub>2</sub>	HVOF	1.04	Present work
TiO <sub>2</sub>	HVOF	1.11(a)	Buchmann and Gadow <sup>[20]</sup>
TiO <sub>2</sub>	APS	0.78(a)	Buchmann and Gadow <sup>[20]</sup>
PSZ	APS	0.78	Lima et al. <sup>[9]</sup>

(a) Ratio calculated by the present author

chanical properties measured via indentation techniques may be affected by very low coating thicknesses.<sup>[3]</sup> This issue must be considered during indentation measurements.

### 3.2 Coating Isotropy

Figures 1 and 2 show that for each specific indentation load (25-1000 g) there is a similarity of both hardness and Weibull modulus values for the top surface and cross-section for the HVOF titania. This characteristic leads to a discussion of coating isotropy. Generally, thermal spray coatings are considered to be strongly anisotropic with respect to the top surface and cross-section due to the mechanism of formation of thermal spray coatings (i.e., spreading and solidification of molten particles). Splats spread parallel to the substrate surface. As a thermal spray coating is formed by a successive overlapping of splats, the resulting microstructure is expected to have different features when examined in parallel (cross-section) or perpendicular (top surface) to the substrate surface. Due to this anisotropic characteristic, engineering books for thermal spray coatings recommend that the hardness values measured on the cross-section should not be compared with values measured on the top surface.<sup>[3]</sup>

Table 2 shows the ratio between Vickers hardness values

measured on the top surface and cross-section of thermal spray ceramic coatings sprayed by HVOF and air plasma spray (APS).<sup>[9,20]</sup> For APS coatings, the hardness of the top surface is about 80% of the cross-section hardness. By comparison the HVOF coatings tend to be more isotropic, having similar values of hardness in the cross-section and top surface.

McPherson<sup>[1,2]</sup> discussed the factors affecting the mechanical properties of APS ceramic coatings. The mechanical properties are determined by the material properties and coarse porosity and are limited by the area of contact between splats (fine pores). An improvement of mechanical properties would be provided by an enhancement in this contact area between splats. The HVOF process generally provides higher impact velocities and denser microstructures than those of the APS process.<sup>[3]</sup> Due to the higher densities, the splat-splat contact should be maximized in HVOF coatings. As a consequence, it is believed that the near isotropic character in the coating mechanical properties observed in the current study is a direct result of the velocity characteristics imparted to the particles in the HVOF process.

Figure 5 shows SEM pictures of the coating microstructure for the top surface and cross-section. The microstructures are somewhat similar, possessing characteristics that differ from the common lamellar structure of many thermal spray coatings. Buchmann and Gadow examined the microstructure of the top surface and cross-section of HVOF and APS titania.<sup>[20]</sup> The top surface and cross-section of the HVOF titania exhibited a homogeneous microstructure, whereas the APS titania contained heterogeneous features for the same regions. Margadant et al. measured properties, such as, electrical resistivity, ultrasound wave speed, and elastic modulus for NiCr coatings sprayed via different thermal spray processes.<sup>[10]</sup> Not surprisingly, that study showed that nearly isotropic microstructures produced nearly the same electrical resistivity, ultrasound wave speed, and elastic modulus for the top surface and cross-section. On the other hand, highly anisotropic microstructures exhibited anisotropic behavior. The experimental observations of this work and Ref. 10 and 20 support the claim that the isotropic behavior in hardness values in the titania coatings arise due to the near isotropic microstructure of the top surface and cross-section of the titania coatings provided by the HVOF process.

### 3.3 Crystallographic Phases

Figure 6 shows the XRD patterns of the titania feedstock and coating. Titania has three polymorphs: low-temperature anatase, brookite, and high-temperature rutile. Anatase and brookite transform irreversibly to rutile at temperatures from 400-1000 °C.<sup>[21]</sup> The starting temperature and rate of this transformation are largely affected by impurities and particle size.<sup>[21]</sup> The spectrum shown in Fig. 6(a) indicates that the process used in producing the titania feedstock resulted in the presence of rutile and some residual phase (TiO<sub>x</sub>) with XRD peaks close to those of anatase and/or brookite. After thermal spraying using HVOF, the coating (Fig. 6b) contained rutile as the major phase and anatase or brookite as a minor phase, represented by their 100% intensity peak at 25.3°. It is assumed that the thermodynamic conditions during the spray process transformed most of the residual phase into rutile and anatase or brookite. No significant degradation of the titania phase was observed; i.e., the coating contained the TiO<sub>2</sub> phase. Buchmann and

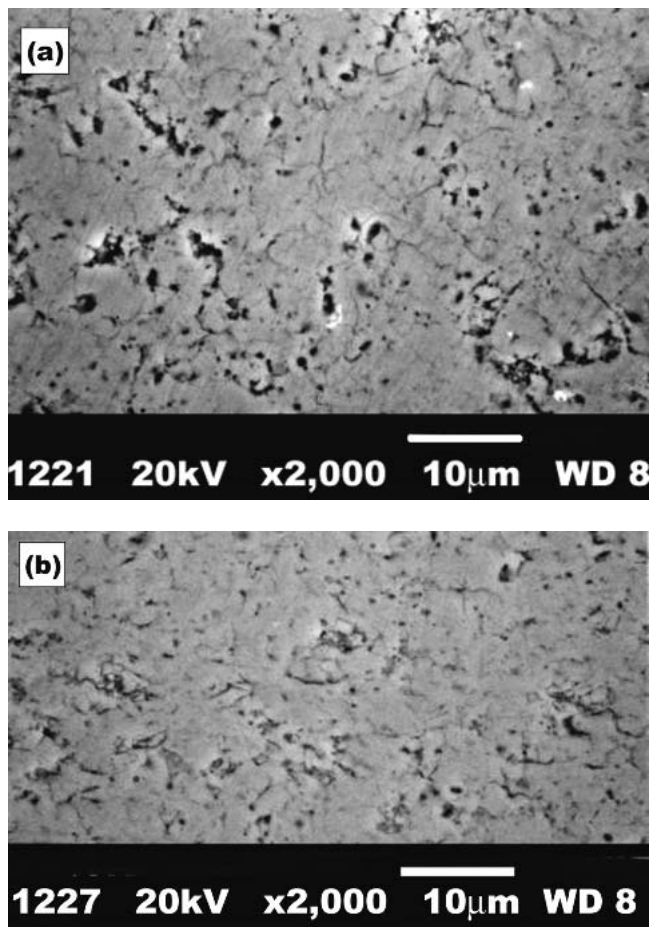


**Fig. 5** (a) Top surface of the HVOF titania coating, (b) cross section of the HVOF titania coating

Gadow observed similar characteristics for HVOF titania.<sup>[20]</sup> This is in contrast to APS titania coatings in which degradation of the  $\text{TiO}_2$  stoichiometry was revealed.<sup>[20]</sup> In that work,<sup>[20]</sup> the  $\text{TiO}_2$  phase was reduced to  $\text{Ti}_4\text{O}_7$  and  $\text{Ti}_7\text{O}_{13}$ , also known as Magnéli phases  $\text{Ti}_n\text{O}_{2n-1}$  ( $n = 4-10$ ).<sup>[21]</sup> The Magnéli phases are formed when  $\text{TiO}_2$  is annealed in a reducing atmosphere.<sup>[21]</sup>

The HVOF process involves lower particle temperatures and higher particle velocities than those attained in APS.<sup>[3]</sup> Ceramic materials are rarely sprayed using HVOF due to their high melting points, lack of plasticity and low thermal conductivities. The data to be presented in the following section indicates that there is a strong probability that many titania particles do not fully melt during the HVOF process. As a consequence, no significant changes in the  $\text{TiO}_2$  stoichiometry were noticed during this work. Buchmann and Gadow speculate that the HVOF process may have an oxidizing effect on the titania, thereby impeding the loss of oxygen that can lead to the formation of the Magnéli phases.<sup>[20]</sup>

### 3.4 In-Flight Particle Characteristics

Figures 7 and 8 show the histograms of temperature and velocity, respectively, for the HVOF sprayed titania particles. The

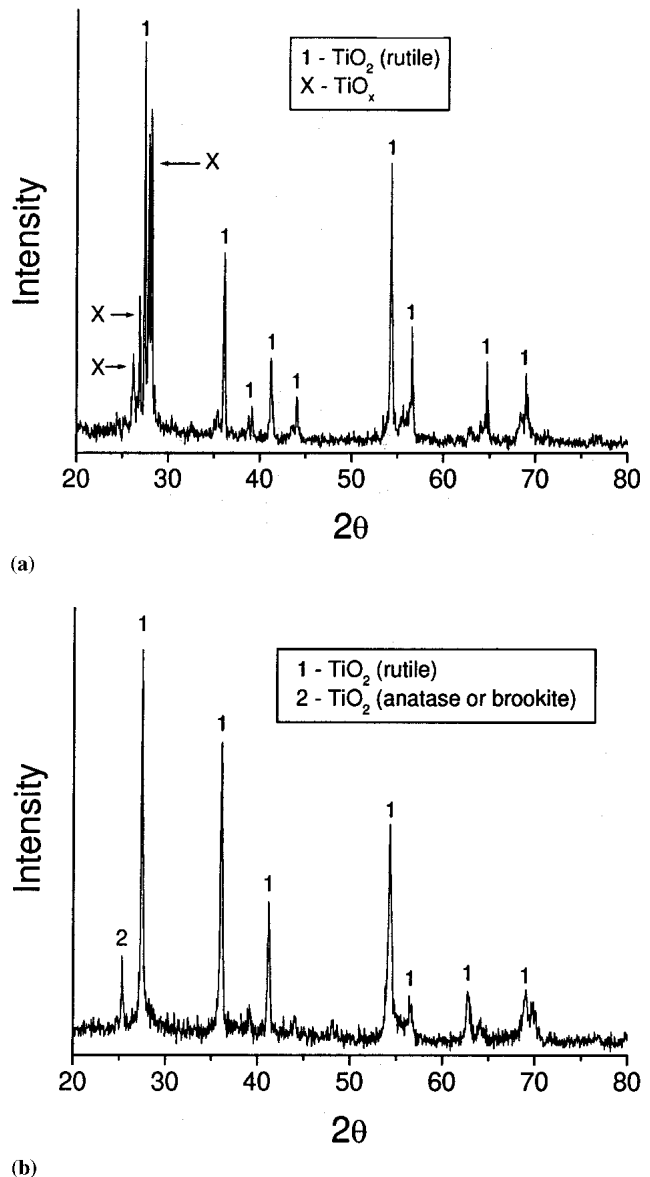


**Fig. 6** (a) XRD pattern of the titania feedstock; (b) XRD pattern of the HVOF titania coating

in-flight particle data were acquired at a spray distance of 20 cm (Table 1), the distance at which the substrate would normally be positioned when depositing a coating. The melting point of titania is  $1855\text{ }^\circ\text{C}$ .<sup>[21]</sup> The majority of the titania particles did not reach the melting point (Fig. 7) or were resolidified in the spray jet before reaching the detector. The average particle temperature at a spray distance of 20 cm was  $1807 \pm 134\text{ }^\circ\text{C}$ , which is approximately  $50\text{ }^\circ\text{C}$  below the melting point noted above. It must be pointed out that an error related to pyrometric calibration may be present in the particle temperature measurements; i.e., the real particle temperature values may be higher or lower than those measured. The velocity behavior exhibits a near Gaussian distribution (Fig. 8) around an average value of  $588 \pm 124\text{ m/s}$ .

Figure 9 shows a graph of particle temperature *versus* particle

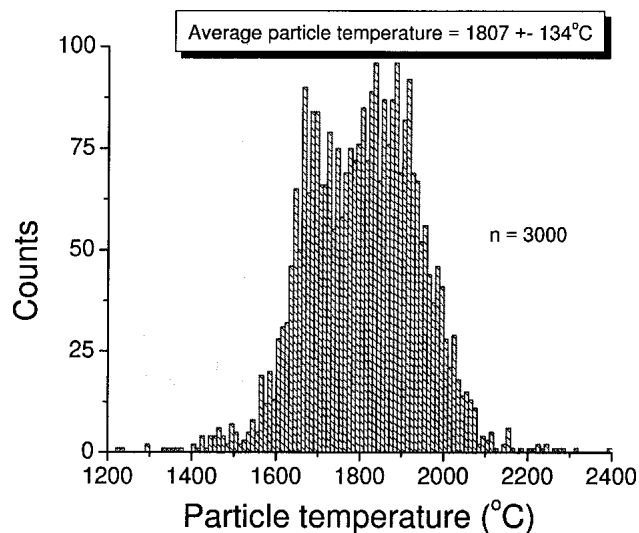


**Fig. 7** Histogram of particle temperature for the HVOF sprayed titania particles

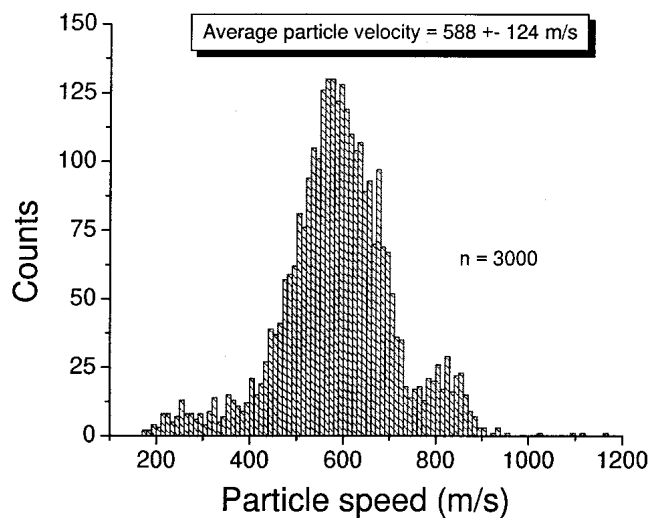


**Fig. 8** Histogram of particle velocity for the HVOF sprayed titania particles

diameter. This graph also reveals that the majority of the sprayed particles did not reach the melting point or were resolidified during the spray process. The titania feedstock used in this study had a nominal particle size distribution varying from 5–22  $\mu\text{m}$ . The majority of the particles detected in the spray jet were found to be in this range (Fig. 9); however, some particles larger than 22  $\mu\text{m}$  were observed. Although it is thought that these large particles were introduced into the feedstock during the sieving process, there may be some contribution to this measurement arising from the pyrometric calibration of the DPV2000. The average particle diameter in the spray jet is  $14 \pm 8 \mu\text{m}$ . Figure 9 is divided into four quadrants by two dashed lines. The dashed line intersecting the particle temperature axis divides particles that have temperatures above and below 1850  $^{\circ}\text{C}$ , which is basically the melting point of titania. The dashed line intersecting the particle diameter axis divides particles into those having di-

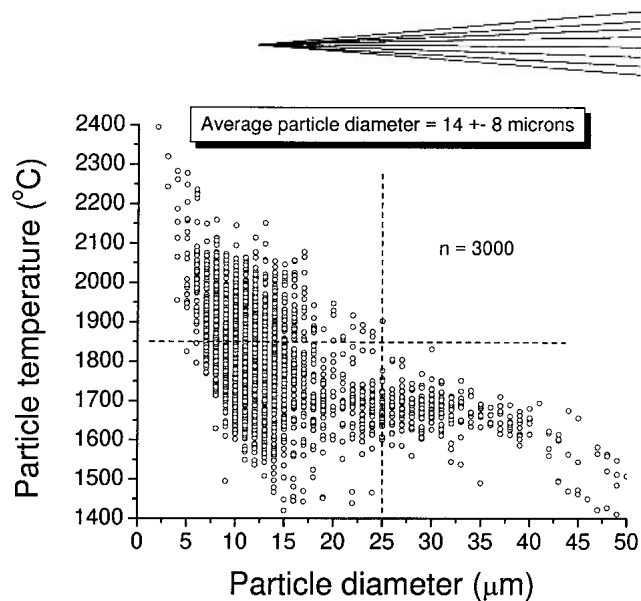


**Fig. 9** Plot of particle temperature vs particle diameter for HVOF sprayed titania particles

ameters above or below 25  $\mu\text{m}$ . No particles larger than 25  $\mu\text{m}$  have temperatures higher than 1850  $^{\circ}\text{C}$ . Therefore, it is assumed that the particles, which are found in the upper left quadrant of Fig. 9, should play the major role in coating formation. Because the particles situated in the other quadrants have temperatures that are lower than the melting point of titania, it is expected that most of them would bounce off the substrate or coating surface. One should notice here that the temperature values represent the temperature at the surface of the particles; i.e., the inner part of the particles may have lower temperatures. Therefore, only the particles located in the upper left quadrant of Fig. 9 should be considered as molten or semi-molten.

The deposition efficiency (DE) during the spraying of this coating was  $\sim 30\%$ . The particles located in the upper left quadrant represent 38% of the total number of particles contained in Fig. 9 ( $n = 3000$ ). This percentage in number of 38% corresponds to a percentage in volume of 8% in relation to the total volume of particles contained in Fig. 9.

Kucuk et al. have observed the same characteristics as those of Fig. 9 when comparing the in-flight particle characteristics with DE values for PSZ particles.<sup>[22,23]</sup> They also demonstrated that PSZ ceramic particles with temperatures lower than that of the melting point do not have an important role in coating formation. This observation demonstrates the lack of plastic behavior of ceramic thermal sprayed particles. It supports the assumption made based on the data of Fig. 9. It is important to point out that this trend was determined for a ceramic powder. Materials that are more susceptible to plastic deformation or forging may present a different trend. Again it is important to emphasize that there is an uncertainty in the measurements of the DPV2000 due to pyrometric calibration issues; i.e., the two dashed lines of Fig. 9 may be somehow shifted from the “exact real values” of particle temperature and diameter. However, this issue does not invalidate the overall experimental data.

### 3.5 Origin of the High Weibull Modulus Values

The HVOF titania coating obtained during this work has higher Weibull modulus values than those found in other ther-

mal sprayed ceramic coatings (Fig. 3). Due to the significant differences of Weibull modulus values between the HVOF titania and the other ceramic coatings (Fig. 3), there is an important opportunity to analyze the processing conditions and microstructural characteristics that led to this coating uniformity. Several factors that may contribute to these results have been identified and are discussed below.

The microstructure of this coating (Fig. 5) does not exhibit the traditional features of lamellar structure. A similar near-uniform microstructure is observed on the top surface and cross section. This characteristic may be one of the causes of the high values of Weibull modulus and also could explain the near isotropic behavior of the hardness.

WC-Co HVOF coatings normally have dense microstructures,<sup>[3]</sup> which should provide coating uniformity. However, the WC-Co HVOF sprayed coatings have low values of Weibull modulus (Fig. 3) compared with HVOF titania. The WC-Co feedstock is composed of two different phases with different properties. When WC-Co is thermally sprayed, due to temperature and environmental effects, other phases can arise in the WC-Co system.<sup>[24]</sup> Increasing the number of phases (different properties) is expected to produce a more heterogeneous system and lower the Weibull modulus. In the current study, the XRD pattern of the HVOF titania (Fig. 6b) identified rutile as the major phase in the coating structure. No other Ti-containing phases having a stoichiometry different from TiO<sub>2</sub> were observed. This phase uniformity may also contribute to producing the high Weibull modulus values.

However, phase uniformity alone is not sufficient to produce high values of Weibull modulus. APS chromia is a single-phase material, but exhibits low values of Weibull modulus (Fig. 3) when compared with HVOF titania. In this case, the typical lamellar APS microstructural characteristics are probably playing a more important role than the single-phase nature of chromia; i.e., the microstructural inhomogeneity of the coating is a more important factor in this case than the compositional homogeneity.

VPS systems tend to produce uniform and homogeneous coatings.<sup>[3,10]</sup> The Weibull modulus values of VPS titania shown in Fig. 3 lie between those of the HVOF titania and the other ceramic coatings. Assuming that the VPS titania coatings contain rutile as the major phase, it is expected that the more uniform microstructure and phase composition should produce a higher Weibull modulus of hardness than observed for the average thermal spray coating. This explanation is consistent with the discussion presented earlier in this section.

The titania feedstock used in this work (Amperit 782.0, H.C. Starck GmbH & Co. KG, Gosler, Germany) has a nominal particle size distribution varying from 5–22  $\mu\text{m}$ . On average, the ceramic powders for thermal spray systems have a particle size distribution varying between 15 and 70  $\mu\text{m}$  (i.e., coarser than that of the Amperit 782.0).<sup>[25]</sup> Feedstocks with a narrow particle size distribution should produce more uniform coatings than those produced from feedstocks with broad particle size distribution. The coefficient of variation values for the overall average particle temperature, velocity, and diameter are 7%, 21%, and 57%, respectively. When analyzing the in-flight characteristics of the particles situated in the upper left quadrant of Fig. 9, the respective values of average temperature, velocity, and diameter (and CV values) are:  $1940 \pm 75$  °C (4%),  $609 \pm 101$  m/s

(17%), and  $10 \pm 3$   $\mu\text{m}$  (30%). As already discussed in Section 3.4, it is assumed that the particles enclosed within the upper left quadrant will play a dominant role in coating formation. The particles located in the upper left quadrant have temperatures higher than that of the melting point of titania. As a consequence, observing the particles located in the upper left quadrant (Fig. 9) and their ranges of temperature and diameter, it is possible to notice that these particles have a uniform particle heating history; which is probably associated with the narrow particle size range ( $10 \pm 3$   $\mu\text{m}$ ). This uniform characteristic in particle heating and diameter may also be important in obtaining coatings with high Weibull modulus.

Due to the low particle temperatures of the HVOF process (when compared with APS), high melting point and lack of plasticity of ceramic materials, the requirement of having a tight particle size control if one intends to spray titania, and probably other ceramic feedstocks, via HVOF systems is of high importance.

Therefore, it is believed that in the current study, a combination of factors contributed to producing coatings having a high Weibull modulus of hardness. These factors included the following aspects: (1) phase uniformity, (2) microstructural uniformity and high density resulting from the particle characteristics produced in the HVOF jet, and (3) narrow particle size range of the feedstock, resulting in a uniform particle heating. It is believed that these aspects merit special attention if the goal is to engineer thermal spray coatings with high Weibull modulus values.

### 3.6 Transition Load-Dependent to Constant Hardness: A New Approach

One may argue that the transition between micro- and macrohardness is located at the transition point where the hardness values do not change with increasing indentation load; i.e., when hardness is independent of load. As discussed in other sections, after a critical indentation load is reached the indentation becomes large enough so that the volume of material being sampled is representative of the bulk. At this point, the various features such as material defects and material composition encountered per unit volume by the indentation become relatively constant.

Finite element modeling (FEM) has been used to engineer and simulate mechanical behavior of thermal spray coatings.<sup>[26,27]</sup> FEM uses 2D and/or 3D computational meshes to model coating response to mechanical inputs. Each computational mesh is formed by an array of elements. The smaller the size of each element, the more accurate is the modeling. It has been shown that coating properties such as hardness and elastic modulus are dependent on dimension (area and/or volume).<sup>[14]</sup> As a consequence, the size of each element in the computer mesh has to take into account this effect to increase the accuracy of the computer model. In their modeling work, Wright et al.<sup>[27]</sup> assumed that all coating properties were homogeneous and isotropic. In that study, the mechanical property values were taken from tabulations for bulk materials. That approach will probably cause the final modeling results to deviate from the experimental ones. Ahmed and Hadfield<sup>[26]</sup> recognized the inhomogeneity effect when modeling thermal spray coatings by investigating the

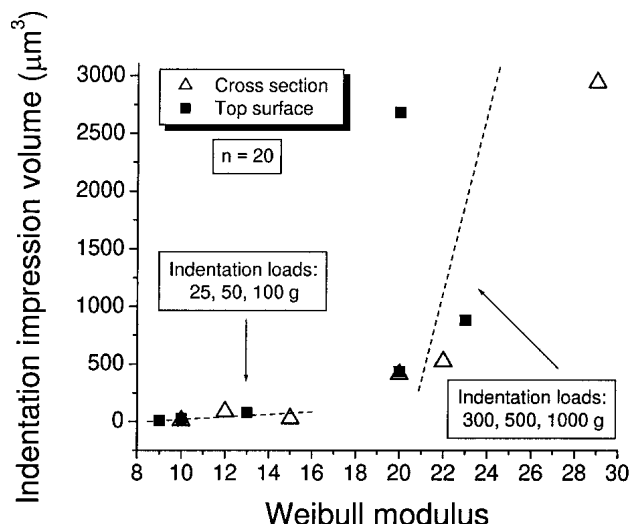


**Fig. 10** Indentation impression volume vs Weibull modulus of hardness for HVOF titania

changing effects in elastic modulus on the location and magnitude of stresses generated in WC-Co coatings.

To increase the accuracy of FEM, it is necessary to determine the dimensions of the microstructural region where material defects encountered per unit area or volume becomes relatively constant; i.e., it is necessary to determine the size of the critical area or volume. In the present work, it is suggested that the size of these dimensions may be obtained by indentation techniques. The size of the element of the computational mesh then may be designed to have its dimensions larger than the critical area or volume. This procedure may improve the performance of FEM and offer more precise computational tools for material scientists and engineers to tailor microstructures.

Figures 10 and 11 show a plot of indentation impression volume and area, respectively, versus Weibull modulus for different indentation loads. The indentation volume and area are taken from the dimensions of the Vickers impression. Each indentation impression was considered as having a square-based pyramid geometry, and the pyramid volume and area were determined for each indentation. Each one of the 12 points of the graph corresponds to the average volume of 20 indentation impressions. The standard deviation values of the data points in Fig. 10 and 11 are not shown due to their very low values relative to the graph dimensions. It is possible to distinguish two data groups. These data groups are represented by two dashed lines included to aid in guiding the eye.

The first data group has a relatively low slope. It represents indentation loads of 25, 50, and 100 g. Within this low-slope group, the indentation impression volume and area are almost constant for significant variations of Weibull modulus. The second data group represents the indentation loads of 300, 500, and 1000 g. This group has a higher slope: the indentation impression volumes and areas change more significantly with lower variations in Weibull modulus values.

It is postulated that the junction between these two groups may represent the transition between micro- and macrohardness. Indentation impression volumes larger than  $\sim 500 \mu\text{m}^3$ , and areas larger than  $\sim 250 \mu\text{m}^2$  may represent the point where material

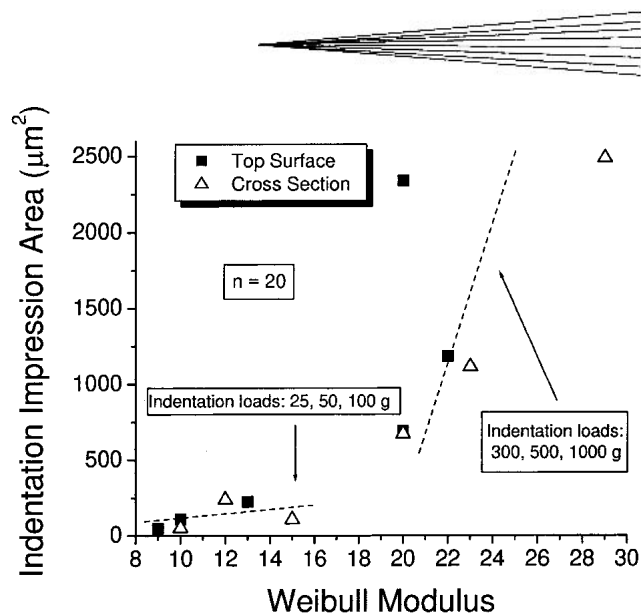


**Fig. 11** Indentation impression area vs Weibull modulus of hardness for HVOF titania

defects encountered per unit volume becomes relatively constant. Figure 1 supports this explanation. After an indentation load in the range of 100-300 g, the hardness values tend to become independent of load; i.e., the transition point apparently has been reached. But this conclusion is based on the observation of average and standard deviation values. As discussed in other sections, average and standard deviation are not sufficient to describe the mechanical properties resulting from the complex thermal spray microstructure. Weibull modulus gives more accurate results, and therefore, the transition point, together with the critical volume or area may be more precisely investigated and determined. In fact, little information can be found in the literature on the transition point between load-dependent hardness and constant hardness. Quinn<sup>[28]</sup> states that the transition point in ceramic materials appears to be associated with the onset of extensive cracking around and underneath the indentation. By comparing the results of Fig. 1 and 10 it may be assumed that the critical load (transition point) in the present case is situated around 300 g, corresponding to a critical volume of  $\sim 500 \mu\text{m}^3$  and a critical area of  $\sim 250 \mu\text{m}^2$ .

Therefore, mechanical properties measured using sampling volumes (or area) equal to or larger than the critical volume (or area) can be used for materials selection and component design or modeling because they represent the overall behavior of the coating or sample being analyzed. Mechanical properties measured in volumes or areas smaller than the critical one may be used for materials selection and component design and modeling if one recognizes that they represent the mechanical behavior of a specific region of the coating, and the necessary adjustments or constraints should be applied.

In addition to the indentation techniques used to measure elastic modulus of materials in localized regions, a new system is being used and developed, the laser ultrasonics technique. Vasquez et al.<sup>[29]</sup> compared the measurements of elastic modulus values of PSZ coatings via laser ultrasonics and Knoop indentation. It was found that the Knoop indentation technique<sup>[15]</sup> was more effective in measuring and representing the elastic modulus values throughout the coating microstructure than the



laser ultrasonics. This difference in effectiveness is probably related to the critical volume. Laser ultrasonics was probably measuring the elastic modulus values in specific regions of the coating, whereas the Knoop indentation was enclosing larger volumes that correspond to the overall microstructure.

It is important to point out that the critical volume and area are approximations. The load used to measure hardness was discrete (Fig. 1) and some degree of elastic recovery of the indentation impression during unloading is an inherent characteristic of the indentation process,<sup>[30]</sup> and it cannot be avoided.

In conclusion, the determination of the critical volume and/or area may be an important piece of information to help in characterizing and understanding thermal spray coatings and bulk samples. Further work on other coatings will be undertaken in the future to gain more insight into the importance of these observations and concepts.

#### 4. Conclusions

Titania coatings produced using HVOF spraying exhibited a near isotropic behavior with respect to the hardness. The origin of this near isotropy is probably related to the characteristics of the HVOF process.

The HVOF titania coatings contained rutile as the major phase. No significant degradation was observed for the TiO<sub>2</sub> stoichiometry. This may result from the partial particle melting, low temperature of the HVOF system, and the oxidizing effect of the oxygen presented in the HVOF flame.

The HVOF titania coatings presented higher Weibull modulus values of hardness when compared with the values for other ceramic thermal spray coatings reported in the literature. The origin of these higher Weibull modulus values is probably a combination of different factors, such as narrow feedstock particle size distribution, the HVOF process, non-lamellar uniform microstructure, uniform particle temperature, and a near single-phase coating.

The Weibull values of hardness of two or more coatings should be compared only if the coatings were indented with the same load. Weibull modulus, like hardness, is load-dependent below the transition point from load-dependent to constant hardness.

The low Weibull modulus values exhibited at low indentation loads (high hardness) are caused due to the small test volume and coating heterogeneity. At high indentation loads (low hardness) the test volume is large, and therefore, there is less scatter in the distribution of data because the influence of material heterogeneity is less.

For the coating evaluated in the current study, the critical load of the transition point between load-dependent and constant hardness is apparently 300 g. It is supposed that at this indentation load a critical volume of  $\sim 500 \mu\text{m}^3$  (and critical area of  $\sim 250 \mu\text{m}^2$ ) is reached. Mechanical properties measured via indentation techniques in volumes larger than  $\sim 500 \mu\text{m}^3$  (and areas larger than  $\sim 250 \mu\text{m}^2$ ) may represent the overall coating behavior and not a particular region of the microstructure; i.e., the point where the number of defects per volume (or area) in the material becomes approximately constant.

These overall results lead to a more general understanding of the relationship between the microstructure, "size effect" of me-

chanical properties, isotropy and coating homogeneity. These findings may help in modeling and prediction of coating microstructure and properties, enabling engineering the microstructure for specific applications.

#### Acknowledgments

The authors want to thank Dr. J.F. Bisson for the scientific curiosity, revision and scientific input in this work. The authors also want to thank F. Belval for HVOF spraying, M. Lamontagne for the DPV2000 measurements, E. Poirier for metallography, and M. Thibodeau for SEM pictures.

#### References

1. R. McPherson: "A Review of Microstructure and Properties of Plasma Sprayed Ceramic Coatings," *Surf. Coat. Technol.*, 1989, 39-40(1-3), pp. 173-81.
2. R. McPherson: "The Relationship Between the Mechanism of Formation, Microstructure and Properties of Plasma-Sprayed Coatings," *Thin Solid Films*, 1981, 83(3), pp. 297-310.
3. L. Pawlowski: *The Science and Engineering of Thermal Spray Coatings*, Wiley, West Sussex, UK, 1995.
4. C.C. Berndt and R. McPherson: "The Adhesion of Plasma Sprayed Ceramic Coatings to Metals, Surfaces and Interfaces in Ceramic and Ceramic-Metal Systems," *Materials Science Research 14*, J. Pask and A. Evans, ed., Plenum Press, New York, NY, 1981, pp. 619-28.
5. P. Ostojic and R. McPherson: "Indentation Toughness Testing of Plasma Sprayed Coatings," *Mater. Forum*, 1987, 10(4), pp. 247-55.
6. C.K. Lin and C.C. Berndt: "Statistical Analysis of Microhardness Variations in Thermal Spray Coatings," *J. Mater. Sci.*, 1995, 30, pp. 111-17.
7. S.H. Leigh, C.K. Lin, and C.C. Berndt: "Elastic Response of Thermal Spray Deposits Under Indentation Tests," *J. Am. Ceram. Soc.*, 1997, 80(8), pp. 2093-99.
8. R.S. Lima, A. Kucuk, and C.C. Berndt: "Bimodal Distribution of Mechanical Properties on Plasma Sprayed Nanostructured Partially Stabilized Zirconia," *Mater. Sci. Eng. A*, 2002, 327, pp. 224-32.
9. R.S. Lima, A. Kucuk, and C.C. Berndt: "Evaluation of Microhardness and Elastic Modulus of Thermally Sprayed Nanostructured Zirconia Coatings," *Surf. Coat. Technol.*, 2001, 135, pp. 166-72.
10. N. Margadant, S. Siegmann, J. Patscheider, T. Keller, W. Wagner, J. Ilavsky, J. Pisacka, G. Barbezat, and P.P. Fiala: "Microstructure—Property Relationships and Cross-Property-Correlations of Thermal Sprayed Ni-Alloy Coatings" in *Thermal Spray 2001—New Surfaces for a New Millennium*, C.C. Berndt, K.A. Khor, and E. F. Lugscheider, ed., ASM International, Materials Park, OH, 2001, pp. 643-52.
11. M. Buchamann and R. Gadow: "Mechanical Characterization of APS and HVOF Sprayed TiO<sub>2</sub> Coatings on Light Metals" in *Thermal Spray 2001—New Surfaces for a New Millennium*, C.C. Berndt, K.A. Khor, and E.F. Lugscheider, ed., ASM International, Materials Park, OH, 2001, pp. 643-52.
12. H. Kurzweg, R.B. Heimann, T. Troczynski, and M.L. Wayman: "Development of Plasma-Sprayed Bioceramic Coatings With Bond Coat Based on Titania and Zirconia," *Biomaterials*, 1998, 19, pp. 1507-11.
13. R.B. Heimann: "Design of Novel Plasma Sprayed Hydroxyapatite-Bond Coat Bioceramic Systems," *J. Therm. Spray Technol.*, 1999, 8(4), pp. 597-603.
14. J.P.P. Singh, M. Sutaria, and M. Ferber: "Use of Indentation Technique to Measure Elastic Modulus of Plasma-Sprayed Zirconia Thermal Barrier Coating," *Ceram. Eng. Sci. Proc.*, 1997, 18(4B), pp. 191-200.
15. D.B. Marshall, T. Noma, and A.G. Evans: "A Simple Method for Determining Elastic-Modulus-to-Hardness Ratio Using Knoop Indentation Measurements," *J. Am. Ceram. Soc.*, 1982, 65(10), pp. C-175-176.
16. T. Valente: "Statistical Evaluation of Vicker's Indentation Test Results for Thermally Sprayed Materials," *Surf. Coat. Technol.*, 1997, 90, pp. 14-20.
17. M. Factor and I. Roman: "Vickers Microindentation of WC-12%Co Thermal Spray Coating, Part 1: Statistical Analysis of Microhardness Data," *Surf. Coat. Technol.*, 2000, 132(2-3), pp. 181-93.
18. C.C. Berndt, J. Ilavsky, and J. Karthikeyan: "Microhardness-Lifetime



- Correlations for Plasma Sprayed Thermal Barrier Coatings” in *Thermal Spray: International Advances in Coatings Technology*, C.C. Berndt, ed., ASM International, Materials Park, OH, 1992, pp. 941-46.
19. J. Karthikeyan, A.K. Sinha, and A.R. Biswas: “Impregnation of Thermally Sprayed Coatings for Microstructural Studies,” *J. Therm. Spray Technol.*, 1996, 5(1), pp. 74-78.
  20. M. Buchmann and R. Gadow: “Mechanical and Tribological Characterization of APS and HVOF Sprayed  $TiO_2$  Coatings on Light Metals” in *Thermal Spray 2001: New Surfaces for a New Millennium*, C.C. Berndt, K.A. Khor, and E. F. Lugscheider, ed., ASM International, Materials Park, OH, 2001, pp. 1003-08.
  21. M. Miyayama, K. Koumoto, and H. Yanagida: “Engineering Properties of Single Oxides” in *Engineered Materials Handbook, 4—Ceramic and Glasses*, S.J. Schneider, ed., ASM International, Materials Park, OH, 1991, pp. 748-57.
  22. A. Kucuk, R.S. Lima, and C.C. Berndt: “Influence of Plasma Spray Parameters on In-Flight Characteristics of  $ZrO_2$ -8wt%  $Y_2O_3$  Ceramic Particles,” *J. Am. Ceram. Soc.*, 2001, 84(4), pp. 685-92.
  23. A. Kucuk, R.S. Lima, and C.C. Berndt: “Influence of Plasma Spray Parameters on Formation and Morphology of  $ZrO_2$ -8wt%  $Y_2O_3$  Deposits,” *J. Am. Ceram. Soc.*, 2001, 84(4), pp. 693-700.
  24. H.L. de Villiers Lovelock: “Powder/Processing/Structure Relationships in WC-Co Thermal Spray Coatings: A Review of the Published Literature,” *J. Therm. Spray Technol.*, 1998, 7(3), pp. 357-73.
  25. Sulzer Metco—The Coatings Company: [www.sulzermetco.com](http://www.sulzermetco.com) (10/23/2001).
  26. R. Ahmed and M. Hadfield: “Rolling Contact Fatigue Behavior of Thermally Sprayed Rolling Elements,” *Surf. Coat. Technol.*, 1996, 82, pp. 176-86.
  27. J.K. Wright, J.R. Fincke, R.N. Wright, W.D. Swank, and D.C. Haggard: “Experimental and Finite Element Investigation of Residual Stresses Resulting From the Thermal Spray Process” in *Advances in Thermal Spray Science & Technology*, C.C. Berndt and S. Sampath, ed., ASM International, Materials Park, OH, 1995, pp. 187-92.
  28. G.D. Quinn: “Hardness Testing of Ceramics,” *Adv. Mater. Proc.*, 1998, 8, pp. 23-27.
  29. D.L. Vasquez, A. Kucuk, R.S. Lima, U. Senturk, and C.C. Berndt: “Elastic Modulus Measurements of Air Plasma Sprayed Yttria Partially Stabilized Zirconia Coatings Using Laser Ultrasonics and Indentation Techniques” in *Thermal Spray 2001: New Surfaces for a New Millennium*, C.C. Berndt, K.A. Khor, and E.F. Lugscheider, ed., ASM International, Materials Park, OH, 2001, pp. 1045-50.
  30. B.R. Lawn and V.R. Howes: “Elastic Recovery at Hardness Indentations,” *J. Mater. Sci.*, 1981, 16, pp. 2745-52.